Hindawi
Journal of Sensors
Volume 2021, Article ID 6108223, 11 pages
https://doi.org/10.1155/2021/6108223

Research Article

Investigation on the Lightning Location and Warning System Using Artificial Intelligence

Tianru Shi,[1] Danhui Hu,[1] Xiang Ren,[1] Zeqi Huang,[1] Yaodong Zhang,[1] and Jianlan Yang[2]

[1]*State Grid Hubei Electric Power Co., Ltd., Research Institute, Wuhan 430077, China*
[2]*College of Electrical & Information Engineering, Hunan University, Changsha 410082, China*

Correspondence should be addressed to Jianlan Yang; yangjianlan@hnu.edu.cn

Received 23 June 2021; Accepted 9 August 2021; Published 6 September 2021

Academic Editor: Ruizhen Yang

An in-depth study on a lighting location system is conducted in this paper. Firstly, the history and application of this system are summarized. The overall structure is detailed, including the detection principle of the lightning location, the orientation method, the detection circuit, the method of discriminating cloud flash and ground lightning signal, the error analysis, the guideline for station deployment, the preprocessing of the central station, and the function and structure of data server and user interface. The development of a lightning monitoring system in China is presented, and the construction of a new generation of a lightning location system in the Hubei Province power grid is introduced. Through the collection of measured data, the performance of the lightning location system in the lightning accident inspection rate, lightning location, and lightning situation statistics are analyzed. Artificial intelligence algorithms are applied in the lightning warning system. The new system has a high predicting accuracy.

1. Introduction

Lightning is a high-intensity electromagnetic pulse phenomenon that frequently occurs in nature [1, 2]. As its impact is huge, it has received extensive attention from many industry fields, such as meteorology, aerospace, aviation, electric power, and petroleum. Among them, the power grid is susceptible to lightning due to its wide-area distribution and a geometric scale of thousands of kilometers [3]. It is estimated that the number of trips on high-voltage transmission lines caused by lightning accounts for 40% to 70% in China. Lightning is an important factor that seriously affects the safe operation of the power grid.

The observation of accurate lightning parameters is the basis for lightning protection [4–6]. The key to detect lightning is the lightning location. It refers to automatic detection equipment, which uses the characteristics of sound, light, and electromagnetic wave radiated by the lightning return strike to remotely measure the discharge parameters [7]. Several methods for detecting lighting have been proposed including acoustic, optical, and electromagnetic field methods [8–10]. The modern lightning location system started in 1976. Krider used a single-chip technique to successfully transform the original double-cathode oscilloscope lightning detector into an intelligent magnetic direction lightning location system, which effectively improved the accuracy of lightning angle measurement. In the early 1980s, the emergence and application of cloud-to-ground lightning waveform identification technology enabled the detection efficiency to reach up to 90%. Since then, all developed countries and regions in the world have begun to install lightning monitoring and location networks, e.g., the United States, Canada, Japan, France, and Germany. In the 1990s, due to the use of the global positioning system (GPS), lightning monitoring added GPS clocks based on a direction finding system to form a time difference direction hybrid system. Meanwhile, the use of digital signal processing (DSP) and integrated technology to perform correlation analysis and position processing on the waveform greatly improves the prediction performance. Currently, there are

more than 60 lightning location system networks worldwide that employ commercial instrumentation operating in the very low frequency/low frequency range.

The lightning location system has been widely used in the aerospace, disaster reduction, and prevention and power industries, especially in the global power system. Over 40 countries in the world have installed lightning monitoring systems. Over the past decades, with the development of science and technology and the continuous improvement of itself, the location accuracy and detection efficiency of the lightning location system have been greatly improved. The current lightning location system uses GPS satellite positioning technology, satellite communications, geographic information system (GIS), and other high-tech technologies to form a real-time dynamic multipurpose large-scale information system.

Extensive research has been done on the statistical analysis of lightning parameters [11, 12]. Chen et al. proposed a grid method based on the huge data accumulated by the lightning location systems and used data mining technology to analyze the temporal and spatial distribution of lightning [13]. An improved grid method using the two parameters of a grid area and observation range is developed to further improve the accuracy. Many scholars have analyzed the influence of region and climate change on lightning parameters [14–17]. The lightning parameters of crucial transmission line corridors are analyzed, reducing the error in the area where the line is located. The influence of lightning current amplitude probabilities on the trip rate of the transmission line is investigated, considering different topography and landforms.

2. Sensing Principle of the Lightning Location System

2.1. Structure of the Lightning Location Station. The detection station is composed of an electromagnetic field antenna, lightning waveform recognition and processing unit, high-precision crystal oscillator and GPS clock unit, communication, power supply, and protection unit [18]. It measures and outputs the characteristic quantities of ground-flash waves: the time, direction, and relative signal strength of each return strike, and sends the original measurement data to the central station in real time. Each part of the detection station has a unique function [19]. The GPS antenna is mainly used to receive a GPS synchronization signal. The electromagnetic antenna is composed of two vertical orthogonal frame antennas for receiving electromagnetic wave signals. The circuit structure of the detection station is shown in Figure 1.

The GPS clock unit is used to provide the required high-precision synchronization time signal. The lightning waveform delay processing circuit and the overrange timing circuit are specially designed to improve the accuracy of electromagnetic wave signal detection and lightning strike location. Meanwhile, a drift calibration is developed to avoid errors caused by the drift of the GPS clock crystal oscillator affected by temperature rise. These devices would improve both the detection efficiency and accuracy.

Each detection station of the lightning location system is equipped with a time difference clock, which is composed of a high-stability constant temperature crystal oscillator, a GPS antenna, and a clock board, as given in Figure 2. The clock consists of a highly stable crystal oscillator. GPS can receive a high-precision second pulse time signal and use this signal to correct the clock. The accuracy and reliability of the revised clock are greatly improved. The quality of the GPS receiving board and antenna is reliable, and the time error is less than $0.5\,\mu$s.

2.2. Directional Location Principle of the Lightning Location System. The lightning is accompanied by strong light, sound, and electromagnetic radiation. Among them, the most suitable signal for detecting in a relatively large range is electromagnetic radiation. The electromagnetic radiation of thunder and lightning mainly spreads along the earth surface through low frequency and very low frequency. The range is several hundred kilometers and sometimes can be wider, which is determined by the discharge energy. When extracting signals, the lightning location system activates multiple detection stations to measure the electromagnetic radiation generated by lightning, eliminate the signal of cloud flashes, and identify ground-to-ground flashes. The antenna can measure signals with a frequency ranging from 1 kHz to 1 MHz. Through the electronic circuit, the ground flashing signal is identified and the peak value of each return wave is sampled. The orientation method is the most widely used in the directional location principle.

It employs the magnetic field intensity to obtain the azimuth of the lightning strike point relative to the detection station. In order to detect the radiation waves of the ground flash magnetic field, as depicted in Figure 3, the two orthogonal antennas are in east-west and north-south directions, respectively. If a lightning strike occurs on A, the orthogonal antenna can receive two magnetic signals of different strengths. Assuming that the measured magnetic field strengths in the east-west and north-south directions are H_{WE} and H_{NS}, respectively, the direction angle of the lightning strike point can be calculated as follows:

$$\tan\alpha = \frac{H_{\mathrm{NS}}}{H_{\mathrm{WE}}}. \tag{1}$$

The angles measured by two detection stations are shown in Figure 4. According to the angle relationship of the triangle, the azimuth of point A is expressed as

$$B = B_1 + \alpha_{1P}^{B}\left(1+\eta_1^2\right)\left(1-\frac{3}{2}\eta_1^2\tan B\,\alpha_{1P}^{B}\right), \tag{2}$$

$$L = L_1 + \sin^{-1}\left[\frac{\sin\alpha_{1P}\sin\beta_{1p}}{\cos\left(\beta_1+\alpha_{1P}^{B}\right)}\right]. \tag{3}$$

In Figure 4, A is the location of the lightning strike, TDF1 and TDF2 are two different detection stations, the coordinates of TDF1 are (B_1, L_1), the coordinates of TDF2

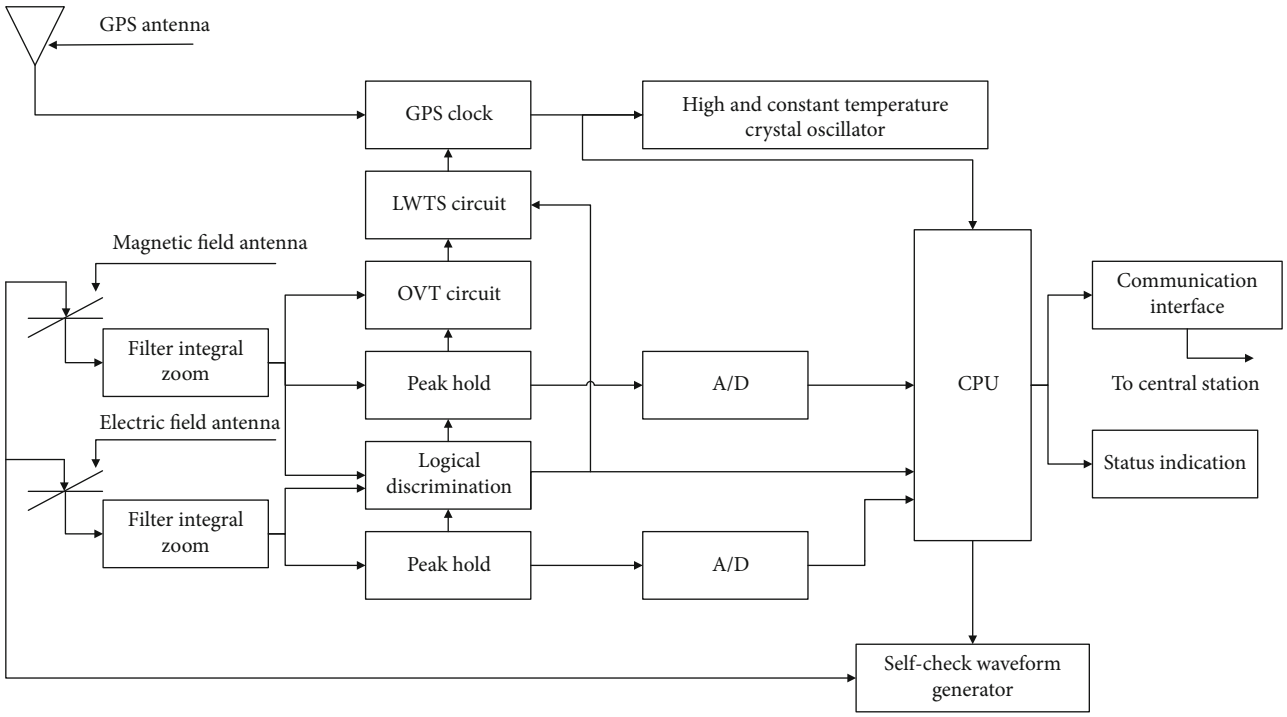

Figure 1: Principle structure of the detection station circuit.

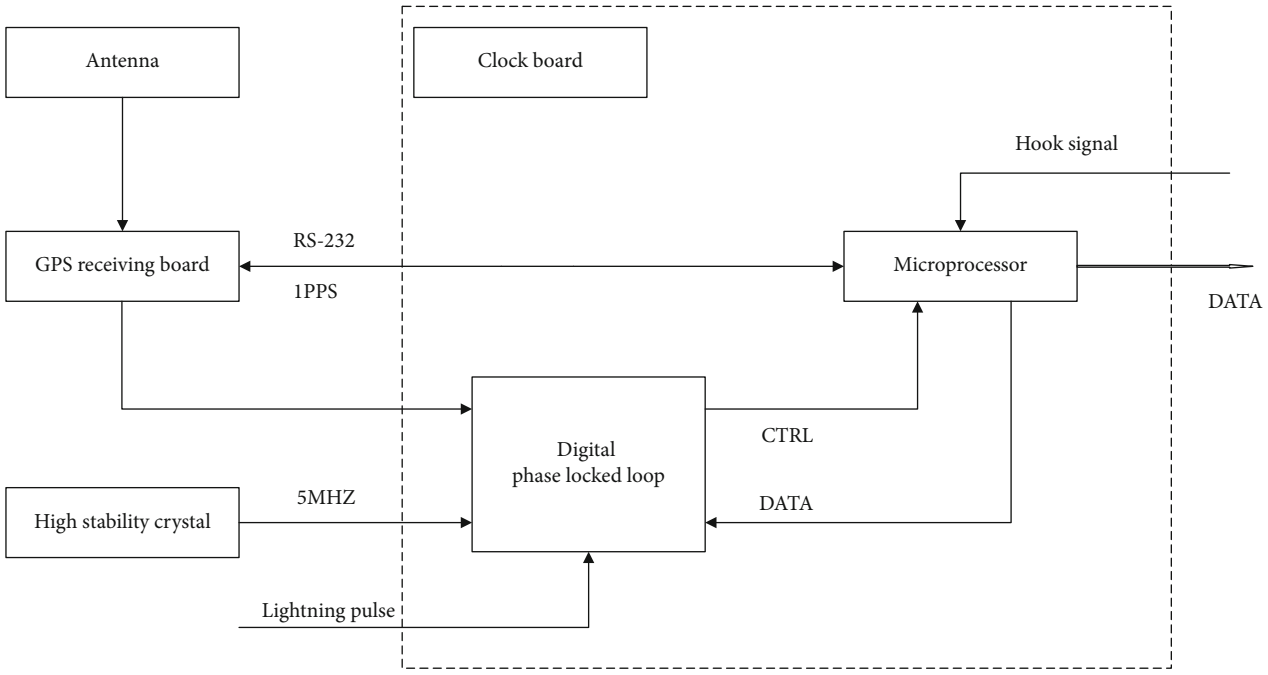

Figure 2: GPS clock unit.

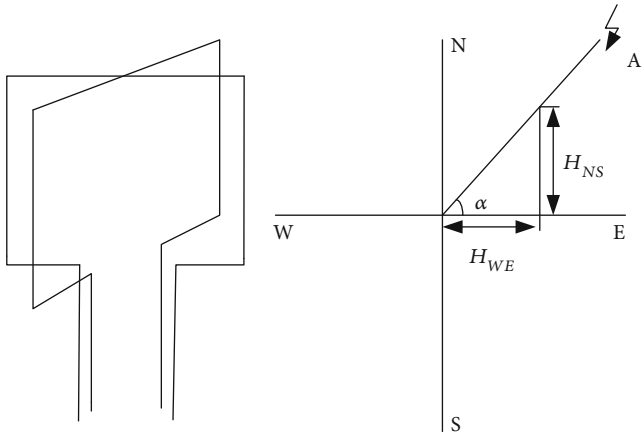

Figure 3: Orientation method.

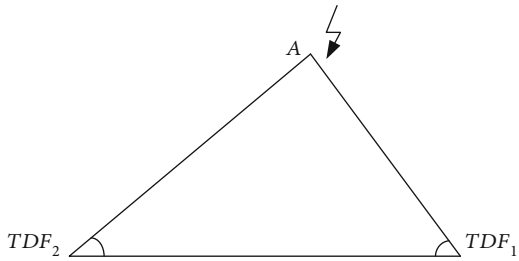

Figure 4: Obtaining the location of lightning strikes by the orientation method.

are (B_2, L_2), B is the latitude, L is the longitude, and β_{1P} and β_{2p} are the azimuth angle.

2.3. Structure of the Lightning Location System. The lightning location system uses a browser/server mode to publish the lightning location information on the web, and its structure is given in Figure 5.

3. Application of the Lightning Location System in the Hubei Power Grid

3.1. Hubei Power Grid Lightning Location System. The lightning location system of the Hubei power grid was established in 1998, with six base stations located in Puqi, Huangshi, Xiaogan, Jingmen, Jingzhou, and Yichang, respectively. In 2000, three stations were added in Suizhou, Xiangfan, and Shiyan, and from 2002 to 2005, five other stations were built in Enshi, Qianjiang, Macheng, Shishou, and Badong. After 13 years of construction and operation, a lightning detection network consisting of 14 lightning detection stations has been developed. Based on the principles of time difference and direction location as well as modern communication technology, the automatic monitor with full real-time function in most areas in Hubei Province has been realized.

More than 1930 transmission lines of various voltage grades in Hubei Province were input into the system. It can be widely used in investigation of the line fault point, lightning parameter statistics, and lightning accident analysis. It reduces the loss of power failure caused by lightning strike and the labor intensity of searching the lightning strike point. The safety of the power system can be ensured.

3.2. Frequency of Lightning Activity in the Hubei Power Grid. From 2014 to 2018, the lightning activity was frequent in Hubei, and the average lightning density in the whole province was between 1.6 and 2.3 times/km^2. In 2018, lightning activity was the most intense, and the density reached 2.29 times/km^2. The lightning activity in Hubei in recent 5 years is listed in Table 1.

Taking 2018 as an example, there were 10 times of the lightning trip in the Hubei power grid for voltage levels of 500 kV and above, including once in March, once in April, thrice in June, quartic in July, and once in August. The most lightning trips were in June and July. The time distribution characteristics of lightning tripping are shown in Figure 6.

In 2018, overhead transmission lines of 500 kV and above were tripped 10 times due to lightning strikes, an increase of 6 times over the same period last year. The lightning density was 2.29 times/km^2, 1.44 times higher than that of the same period last year, which was the highest in the past five years. The results of ground lightning density and lightning trip times are shown in Figure 7. The number of lightning strikes increases with the rise of lightning density.

Compared with the lightning density map in 2017, the lightning activity is changed significantly in 2018. In 2017, the areas with high lightning density were mainly concentrated in the southern part of Jingzhou, Huangshi, Huanggang, and Xianning. In 2018, a large area of C1 level regions appeared in central Yichang, Jingzhou, Jingmen, Shiyan, and Wuhan, as shown in Figure 8.

220 kV Hubei Qiaoshun line fault analysis: on July 31, 2012, 220 kV Qiaoshun line was tripped and the reclose was successful. There were obvious discharge traces on both the left front and the right back of ground wire of the #017 pole. In the large side of the middle phase (phase C), the internal string porcelain insulators and connecting fittings had obvious discharge traces. The other poles passed ground and pole climbing inspection, and no abnormality was found. During the fault inspection, it was found that around 15:30-22:00 of July 31, strong lightning and heavy rain began to appear in the area. The lightning information query system is shown in Table 2: within 5 minutes before and after 21:21 on July 31, there were 4 lightning strikes along the second circuit of 220 kV Qiaoshun, and the lightning current amplitude was from -3.4 kA to -18.5 kA, distributed near #016~#020 towers.

After inspecting the transmission tower, the faulty section was located in the vegetable garden in Baijiawan Village, Xiangyang. The line right-of-way was in good condition, without tree barriers, external damage traces, industrial pollution sources, and fouling on insulator strings. There was no strong wind or abnormal local air flow during the fault, and possibilities caused by wind deviation, external damage, pollution, and tree barriers were ruled out, and it was judged

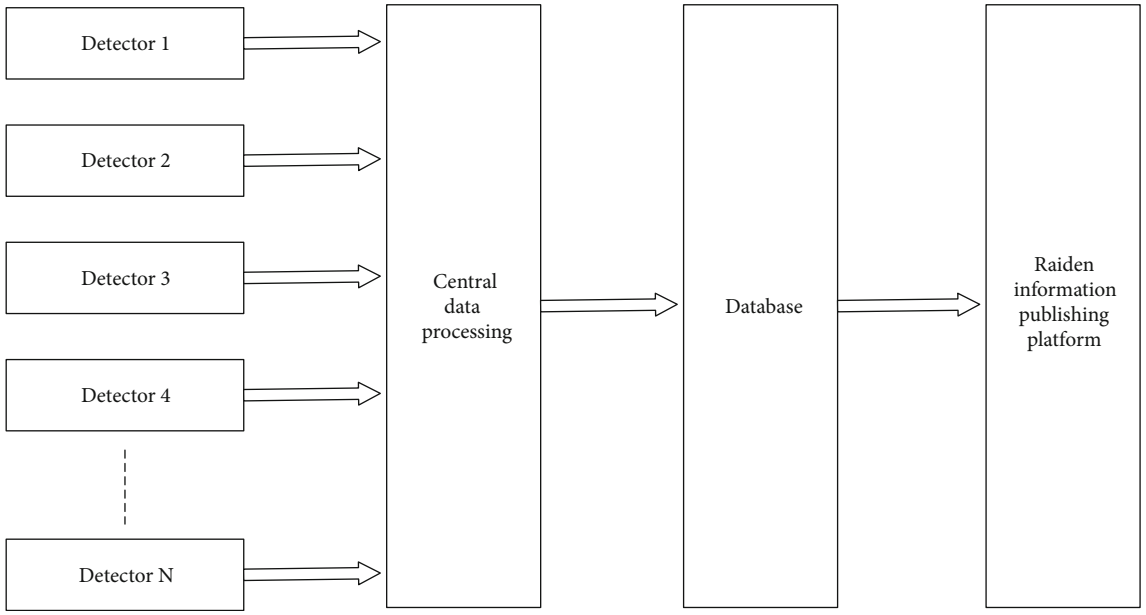

Figure 5: Structure of the lightning location system.

Table 1: Statistics of lightning parameters in Hubei from 2014 to 2018.

Years	Thunder day	Density (times/km^2)	Positive number	Negative number	Positive density (times/km^2)	Negative density (times/km^2)
2014	293	1.7	60419	257572	0.3	1.4
2015	320	2.1	93267	303948	0.5	1.6
2016	256	1.7	82627	236089	0.4	1.3
2017	213	1.6	59874	201418	0.3	1.3
2018	247	2.3	103148	321648	0.6	1.7

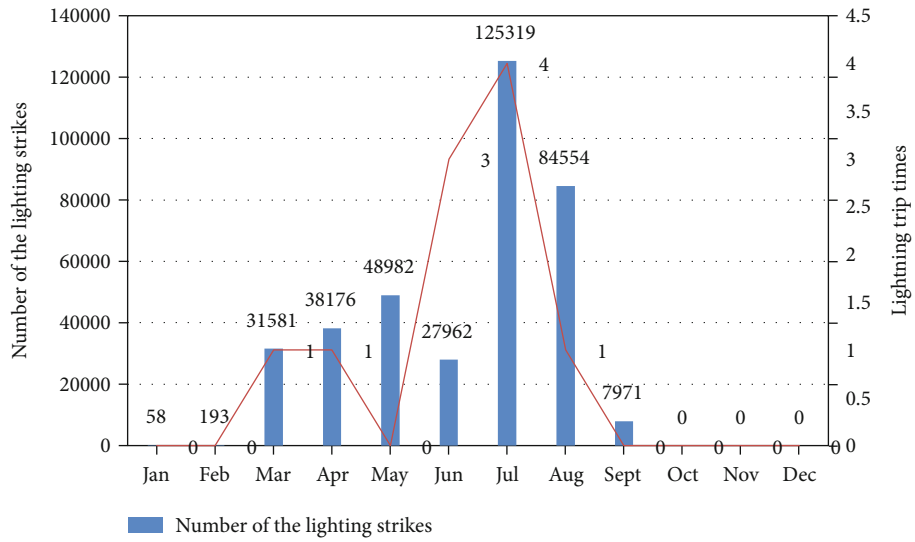

Figure 6: Lightning frequency and lightning tripping frequency of the Hubei power grid.

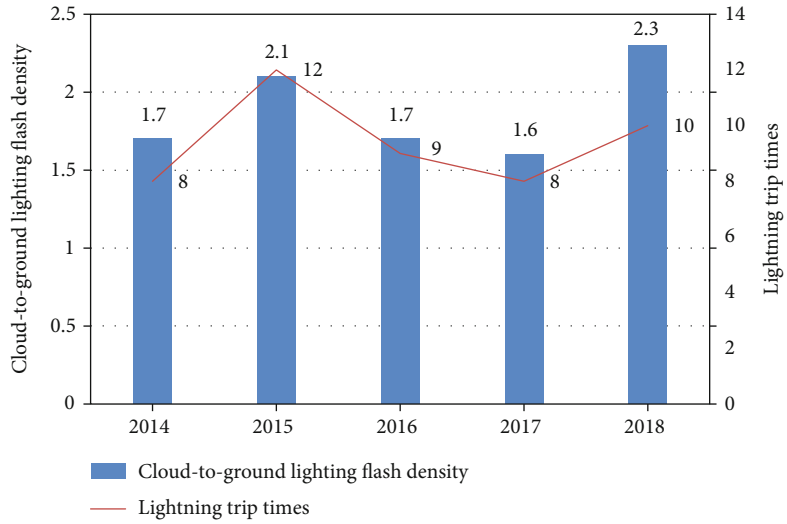

Figure 7: Tripping data of 500 kV and above voltage level lines in the Hubei power grid.

as a lightning fault, line fault scene photo as shown in Figure 9.

4. Application of Artificial Intelligence in the Lightning Warning System

4.1. Principle of Lightning Warning. The key of the lightning warning system is the thunderstorm forecast model, which can send out the lightning warning information in advance and effectively avoid the damage caused by lightning strike to the staff and equipment in the protected area. Thunderstorm prediction is based on a subjective and objective prediction algorithm. Subjective forecast takes observations from Doppler weather radar and combines them with other meteorological satellite cloud maps. The objective algorithms include radar echo or cloud image extrapolation and severe convective weather recognition [20]. However, the success rate of forecast and warning is quite limited. The advancement of big data and artificial intelligence technology, massive historical lightning data, and other meteorological monitoring data are processed and modeled through a deep learning method. As a result, a more accurate local lightning warning model is obtained. In practice, most warning methods are based on the data of the lightning location and atmospheric electric field. The electric field meter is used to determine the lightning probability by measuring the intensity and change trend of the atmospheric electric field, so that different alarm levels can be determined by setting the proper threshold. Under different alarm levels, contingency plans are made to implement actions such as stopping sending and receiving oil to achieve the purpose of active lightning protection.

4.2. Lightning Warning Model. The data of the lightning warning model comes from a 3D lightning locator and other meteorological observation data such as meteorological radar cloud image. The 3D lightning locator is a high-precision system for locating lightning strikes and lightning within clouds. The average detection accuracy is about 300 m, and the detection efficiency is up to 95%. The lightning locator is used to collect the lightning location data within the region, including the time, the location (latitude and longitude information), the height of lightning from the ground, and other attribute information. The XGB (Extreme Gradient Boosting) algorithm is used to build a scoring model for the occurrence probability of lightning strike in the protected area to solve the problem of 0-2-hour approaching warning. The model structure is shown in Figure 10.

A_n is the n basic feature data. An XGB lightning prediction model is built based on the data, and the output is the probability of lightning strike in the surveillance area (the probability value between 0 and 1).

4.3. Feature Extraction. After obtaining the relevant lightning data, it is necessary to extract the data features. According to the periodicity, instantaneity, and mobility of lightning, the following targeted features were extracted from the collected data sources:

(1) Thunderstorm proximity: the distance between the thunderstorm cluster and the protection point

(2) Total number of lightning at close range

(3) Thunderstorm approaching speed in the protected area: the speed of the nearest thunderstorm group approaching the protected area

(4) The increasing trend of lightning strikes: the increasing trend of thunderstorm cluster energy in the presentation window

4.4. Model Training and Evaluation. After completing the selection of characteristic values required for model training, the next step is to use a characteristic variable to train the model and get the best parameters. XGB is used for data

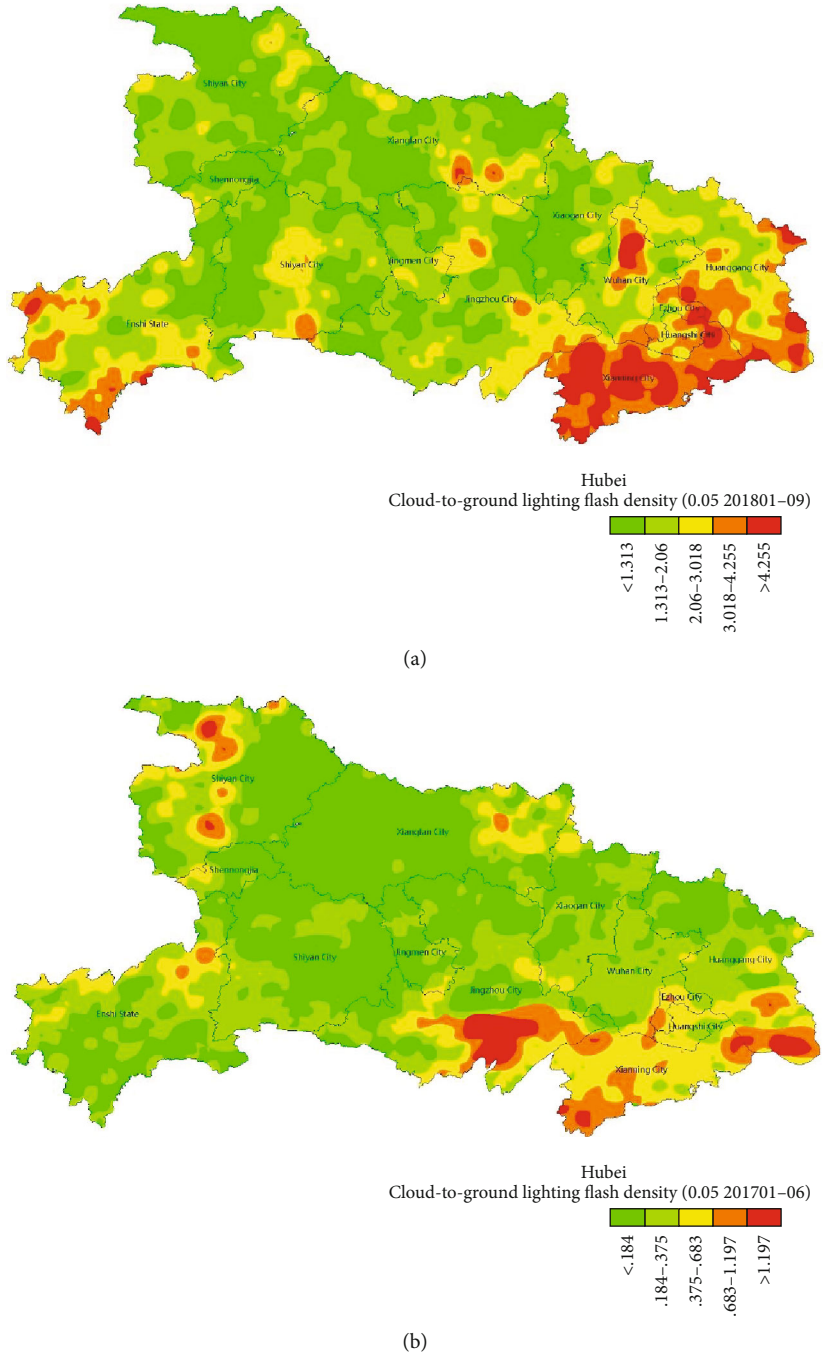

Figure 8: Lightning density distribution in Hubei: (a) 2018 year and (b) 2017 year.

Table 2: Query results of the lightning location system of the Hubei power grid.

Number	Time	Longitude	Latitude	Current (kA)	Reply
1	21:18:54	112.0387	32.0604	-6.3	1
2	21:20:56	112.0521	32.0515	-14.5	1
3	21:21:48	112.0269	32.0737	-18.5	1
4	21:23:26	112.0403	32.0732	-3.4	-1

classification with machine learning integration, and the XGB algorithm structure is shown in Figure 11.

XGB is based on the gradient lifting decision tree (GDBT), which reduces the complexity of the model and avoids overfitting by adding a regularization term into the objective function. The objective function is

$$\text{Obj} = \sum_i l(\hat{y}_i, y_i) + \sum_k \Omega(f_k) + c, \tag{4}$$

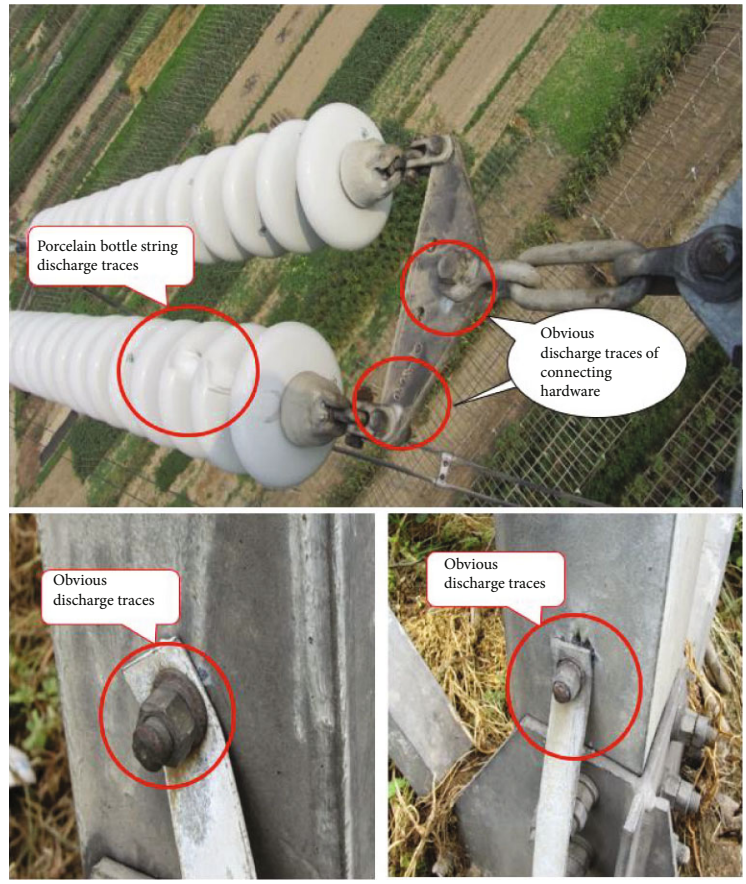

Figure 9: Photo of the line fault scene.

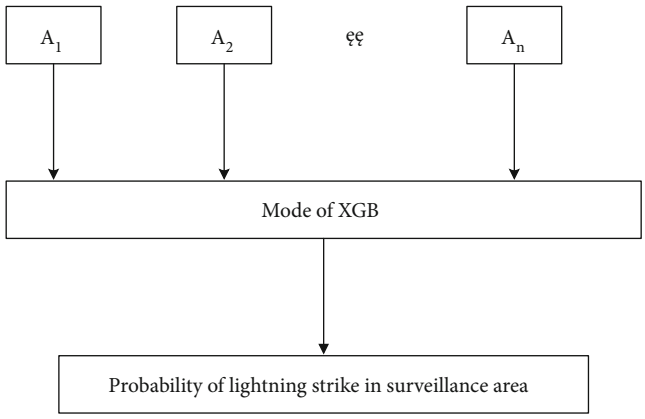

Figure 10: Lighting warning model.

$$\Omega(f_k) = \gamma T + \frac{1}{2}\lambda\|\omega\|^2 = \gamma T + \frac{1}{2}\lambda\sum_{j=1}^{T}\omega_j{}^2, \tag{5}$$

where $\hat{y}_i$ is the predicted value, y_i is the actual value, and l is the loss function, which shows the residual value between the predicted value and the real value. $\Omega(f_k)$ shows the complexity of the model. f_k is the k^{th} decision tree. γ and λ represent the penalty coefficient of the model. T and ω are the number and the weight of leaves for the k^{th} tree, respectively. c is a constant. It is relatively simple to solve the optimal solution for the general least square loss. However, when it is replaced by other loss functions [15], the solution process will become more complex. To solve this problem, the XGB algorithm performs second-order Taylor expansion on this basis. Assume that the t^{th} loss function is defined as

$$\text{Obj}^{(t)} = \sum_i l\left(y\wedge_i{}^{(t-1)}, y_i + f_t(x_i)\right) + \Omega(f_t). \tag{6}$$

The second-order Taylor expansion of formula (6) is carried out, and formula (7) is simplified by removing the constant term.

$$\text{Obj}^{(t)} = \sum_{i=1}^{n}\left[g_i f_t(x_i) + \frac{1}{2}h_i f_t(x_i)^2\right] + \Omega(f_t). \tag{7}$$

Here,

$$\begin{cases} g_i = \partial_{\hat{y}_i(t-1)} l\left(y_i, y\wedge_i{}^{(t-1)}\right), \\ h_i = \partial^2_{\hat{y}_i(t-1)} l\left(y_i, y\wedge_i{}^{(t-1)}\right). \end{cases} \tag{8}$$

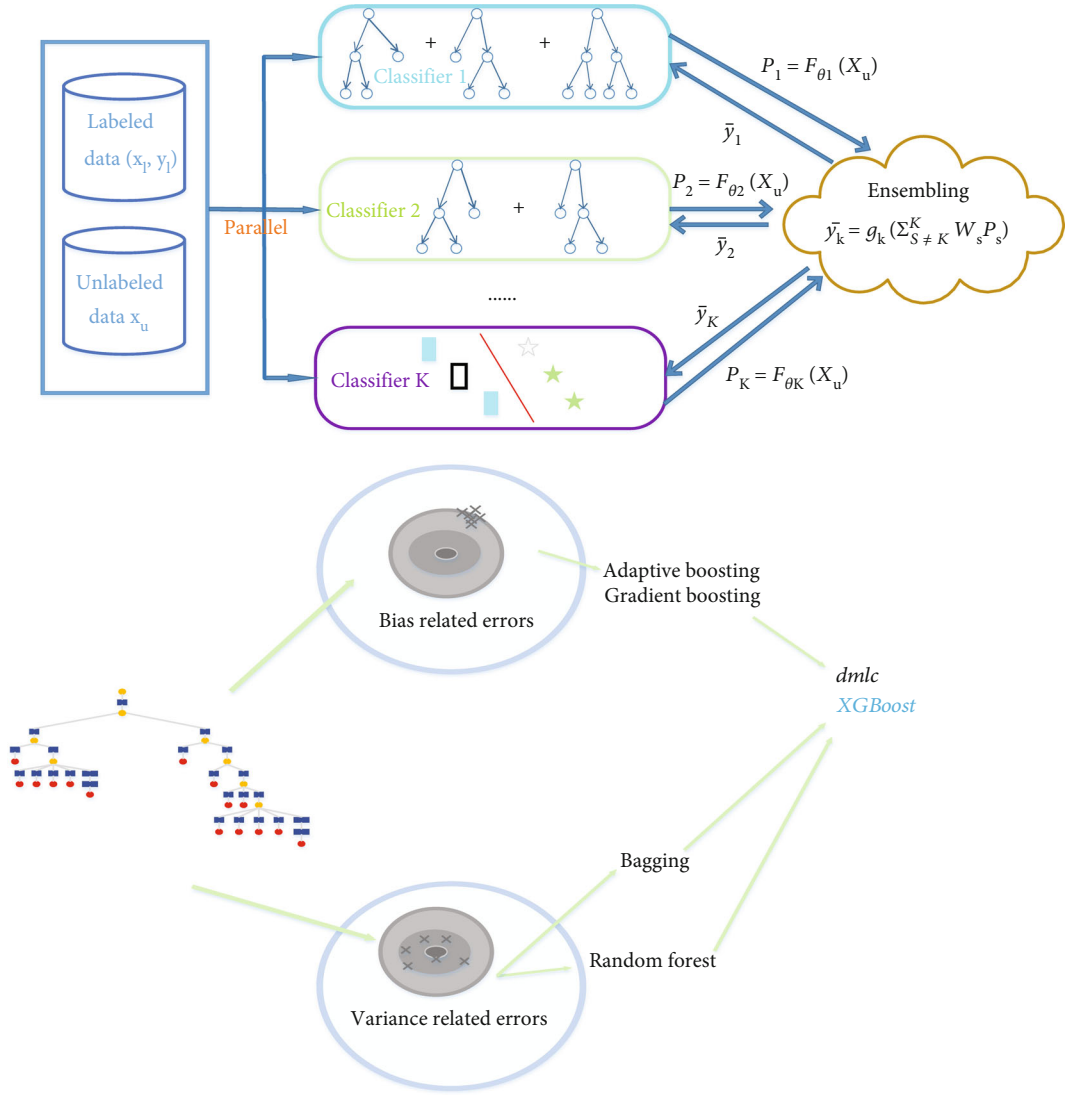

Figure 11: XGB algorithm structure.

The objective function is

$$\begin{aligned} \mathrm{Obj}^{(t)} &= \sum_{i=1}^{n}\left[g_i f_t(x_i) + \frac{1}{2}h_i f_t(x_i)^2\right] + \gamma \mathrm{T} + \|\omega\|^2 \\ &= \sum_{j=1}^{n}\left[\left(\sum_{i\in I_j} g_i\right)\omega_j + \frac{1}{2}\left(\sum_{i\in \mathrm{I}_i} h_i + \lambda\right)\omega_j^2\right] + \gamma T, \end{aligned} \tag{9}$$

where $I_j = \{i|q(x_i) = j\}$ represents the j^{th} group of leaf nodes. At this time, the objective function is transformed into the problem of seeking the minimum of the element quadratic equation on ω_j. Assume that the tree structure is fixed. The optimal weight of leaf node j is in

$$\omega_j = \frac{G_i}{H_j + \lambda}. \tag{10}$$

Then, the objective function is expressed as

$$\mathrm{Obj}^* = -\frac{1}{2}\sum_{j=1}^{T}\frac{G_j^{\ 2}}{H_j + \lambda} + \lambda T. \tag{11}$$

Here,

$$\begin{cases} G_j = \sum_{i\in I_j} g_i, \\ H_j = \sum_{i\in I_j} h_i. \end{cases} \tag{12}$$

Obj $*$ represents the structure score of the regression tree. The smaller the value, the better the structure. Since the structure of all the trees cannot be listed, the greedy algorithm is used for the division of subtrees. Each attempt is made to add a division point to the existing leaf node. The feasible division points are listed, and the division point with

the smallest objective function and the largest gain is selected [16]. The gain formula is given in

$$\text{Gain} = \frac{1}{2}\left[\frac{G_L{}^2}{H_L+\lambda} + \frac{G_R{}^2}{H_R+\lambda} - \frac{G_L+G_R}{H_L+H_R+\lambda}\right] - \gamma. \quad (13)$$

After the XGB model integrates several regression trees, the nodes of each tree are doing feature splitting. The number of times a feature is selected as a split feature can be used as the importance.

After the model training, the model evaluation index is the AUC (Area Under ROC Curve) value and ROC (Receiver Operating Characteristic) curve. Based on the data of the lightning location and other meteorological observation, the AUC value of the model reached 0.95 and the best performance was 1, indicating that the model has a good classification effect. AUC is the area of the ROC curve, which is used to evaluate the quality of the dichotomy system.

$$\text{AUC} = \int_{-\infty}^{+\infty} y(t)dx(t), \quad (14)$$

where x and y are the false-positive rate and true-positive rate, respectively, and also the horizontal and vertical coordinates of the ROC curve.

5. Conclusion

The conclusions are drawn as follows.

(i) The charge distribution of thunderstorm, the density and pressure level of air, and the topography and geological conditions are various in different climatic and geographical areas. In order to improve the accuracy and performance evaluation of the lightning location system, it is necessary to strengthen the observation of natural lightning in different areas

(ii) The cause of a typical lightning fault for a 500 kV transmission line is analyzed in this paper. Several lightning protection measures are introduced. Currently, the lightning protection methods available for transmission lines cannot completely eliminate the impact of lightning. In recent years, extreme weather occurred frequently and there are great uncertainties in lightning activity. It is necessary to further study climate change and lightning behavior

(iii) The lightning warning system can send out the lightning warning information in advance and effectively avoid the damage caused by lightning strike to the staff and equipment in the protected area. The use of artificial intelligence algorithms in the lightning warning system can improve the predicted accuracy

Data Availability

The lightning sensing, location, and warning data used to support the findings of this study were supplied by Hubei Electric Power Company Research Institute under license and so cannot be made freely available. Requests for access to these data should be made to Tianru Shi (739601030@qq.com).

Conflicts of Interest

The authors declare no conflict of interest.

Authors' Contributions

T. Shi and D. Hu proposed the concepts and ideas. X. Ren analyzed the results. Y. Zhang and J. Yang wrote this paper and revised the contents of this manuscript.

Acknowledgments

This work is financially supported by Hubei Electric Power Company (State Grid under Grant No. SGHBDK00SBJS1900425).

References

[1] L. Cai, J. Wang, Q. Li, and Y. Fan, "The Foshan Total Lightning Location System in China and its initial result, presented at the 10th Asia-Pacific," in *Conf. Lightning Protection (APL 2017)*, Krabi, Thailand, 2017.

[2] L. Cai, X. Zou, J. Wang, Q. Li, M. Zhou, and Y. Fan, "The Foshan Total Lightning Location System in China and its initial operation results," *Atmosphere*, vol. 10, no. 3, p. 149, 2019.

[3] R. K. Said, U. Inan, and K. Cummins, "Long-range lightning geolocation using a VLF radio atmospheric waveform bank," *Journal of Geophysical Research*, vol. 115, no. D23, 2010.

[4] P. W. Casper and R. B. Bent, "Results of the LPATS USA national lightning detection and tracking system for the 1991 lightning season," in *21st International Conference on Lightning Protection*, Berlin 1992, 1992.

[5] V. Cooray, Ed., *Lightning Protection, IET Power and Energy Series 58*, The Institution of Engineering and Technology, London, UK, 2010.

[6] IEC technical committee-88, *IEC 61400-24 Wind Turbines-Part 24: Lightning Protection*, International Standard IEC, Geneva, CH, 2010.

[7] A. C. L. Lee, "An experimental study of the remote location of lightning flashes using a VLF arrival time difference technique," *Quarterly Journal of the Royal Meteorological Society*, vol. 112, no. 471, pp. 203–229, 1986.

[8] P. M. Lo, *A Simplified Model for Lightning Exposure of Wind Turbines, Master's Thesis*, McGill University, Montreal, 2008.

[9] V. Cooray, U. Kumar, F. Rachidi, and C. A. Nucci, "On the possible variation of the lightning striking distance as assumed in the IEC lightning protection standard as a function of structure height," *Electric Power Systems Research*, vol. 113, pp. 79–87, 2014.

[10] R. Rodrigues, V. Mendes, and J. Catalão, "Estimation of lightning vulnerability points on wind power plants using the

rolling sphere method," *Journal of Electrostatics*, vol. 67, no. 5, pp. 774–780, 2009.

[11] M. Becerra, M. Long, W. Schulz, and R. Thottappillil, "On the estimation of the lightning incidence to offshore wind farms," *Electric Power Systems Research*, vol. 157, pp. 211–226, 2018.

[12] N. Yang, Q. Zhang, W. Hou, and Y. Wen, "Analysis of the lightning-attractive radius for wind turbines considering the developing process of positive attachment leader," *Journal of Geophysical Research: Atmospheres*, vol. 122, no. 6, pp. 3481–3491, 2017.

[13] J.-H. Chen, Q. Zhang, W.-X. Feng, and Y.-H. Fang, "Lightning location system and lightning detection network of China power grid (in Chinese)," *High Voltage Eng*, vol. 34, pp. 425–431, 2008.

[14] J. Jerauld, V. A. Rakov, M. A. Uman et al., "An evaluation of the performance characteristics of the U.S. National Lightning Detection Network in Florida using rocket-triggered lightning," *Journal of Geophysical Research*, vol. 110, no. D19, article D19106, 2005.

[15] A. Mäkelä, *Thunderstorm Climatology and Lightning Location Applications in Northern Europe*, PhD Thesis, University of Helsinki, Finland, 2011.

[16] A. Mäkelä, T. J. Tuomi, and J. Haapalainen, "A decade of high-latitude lightning location: effects of the evolving location network in Finland," *Journal of Geophysical Research*, vol. 115, no. D21, 2010.

[17] A. T. Pessi, S. Businger, K. L. Cummins, N. W. S. Demetriades, M. Murphy, and B. Pifer, "Development of a long-range lightning detection network for the Pacific: construction, calibration, and performance," *Journal of Atmospheric and Oceanic Technology*, vol. 26, no. 2, pp. 145–166, 2009.

[18] W. Schulz and G. Diendorfer, *Detection Efficiency and Site Errors of Lightning Location Systems*, USA, International Lightning Detection Conference, Tucson Arizona, 1996.

[19] V. Cooray and R. E. Orville, "The effects of variation of current amplitude, current risetime, and return stroke velocity along the return stroke channel on the electromagnetic fields generated by return strokes," *Journal of Geophysical Research*, vol. 95, no. D11, pp. 18617–18630, 1990.

[20] W. Schulz and M. M. F. Saba, "First results of correlated lightning video images and electric field measurements in Austria," in *X International Symposium on Lightning Protection (SIPDA)*, Curitiba, Brazil, 2009.